Highly Potent Irreversible Inhibitors of Neutrophil Elastase Generated by Selection from a Randomized DNA−Valine Phosphonate Library

Josephine Charlton, Gary P. Kirschenheuter, and Drew Smith*

NeXstar Pharmaceuticals, Inc., 2860 Wilderness Place, Boulder, Colorado 80301

Received October 25, 1996; Revised Manuscript Received January 13, 1997[⊗]

ABSTRACT: We incorporated a phosphonate irreversible inhibitor of neutrophil elastase into a randomized DNA library and, using the SELEX process, iteratively selected these assemblies for the most potent elastase inhibitors. The inhibitors were selected against purified elastase and against secreted elastase in the presence of activated neutrophils. Very active aptamer inhibitors were obtained by both methods, with second-order rate constants for inactivation of human neutrophil elastase ranging $(1-3) \times 10^8$ M^{-1} min^{-1}. These rates exceed those of any reported irreversible inhibitor of elastase and exceed the previous best phosphonate inhibitors by 80-fold. The selected inhibitors are also significantly more potent than α-1 proteinase inhibitor in blocking degradation of elastin by activated neutrophils. In contrast to a previous experiment [Smith et al. (1995) *Chem. Biol. 2*, 741−750], a single-enantiomer form of the valyl phosphonate was used rather than a racemic mixture. Our analysis shows that this use of a chirally resolved valyl phosphonate results in selection of much more potent inhibitors and that these inhibitors specifically potentiate a single enantiomeric form of the phosphonate.

Neutrophil elastase (NE)[1] is a highly active serine protease that is capable of degrading a variety of proteins. Stored in azurophilic granules, it is secreted into the extracellular space in response to inflammatory stimuli. NE is thought to participate in disease resistance by facilitating the degradation and phagocytosis of pathogenic bacteria (Birrer, 1993). Because of its ability to also degrade host proteins, including fibronectin and lung elastin, NE activity normally is tightly controlled in order to avoid injury to host connective tissue (Doring, 1994; Gadek, 1992; Kramps et al., 1991; Umeki et al., 1988). One level of control is mediated through the endogenous serine protease inhibitor α-1 PI, which is present in normal plasma at concentrations of ca. 10^{-5} M.

The escape of NE from this regulation has been implicated in a number of pathological states and diseases, including emphysema, cystic fibrosis, idiopathic pulmonary fibrosis, ARDS, ischemia-reperfusion injury, and rheumatoid arthritis (Doring, 1994; Jochum et al., 1993; Powers et al., 1993; Repine, 1992). Changes in the protease−antiprotease balance, on both the micro- and macroscopic scales have been invoked to account for the destructive effects of NE activity (Birrer, 1993; Donnelly et al., 1995; Hubbard et al., 1991; Kramps et al., 1991; Ossanna et al., 1986).

The development of NE inhibitors as therapeutic agents has been pursued by a variety of strategies, including the identification and production of endogenous inhibitors and the synthesis and screening of smaller organic molecules (Edwards & Bernstein, 1994). The synthetic inhibitors include mechanism-based irreversible inhibitors. Serine proteases form a transient covalent complex between the active-site serine and the substrate peptide acyl carbon (hNE prefers valine at this site). Mechanism-based inhibitors form a stable version of this complex, thereby inactivating the enzyme. The development of irreversible inhibitors as therapeutics has been limited by concerns over their specificity: highly active inhibitors tend to be more chemically reactive, causing them to cross-react with other nucleophilic compounds, which of course are at much higher aggregate concentration than the target enzyme. These potential cross-reactions would act to lower the potency of the inhibitor and could also induce toxic side effects.

We recently reported the identification and characterization of RNA-based irreversible inhibitors of human NE, by a process we term "blended SELEX" (Smith et al., 1995). SELEX is a method of identifying nucleic acid sequences that have desirable properties by using a process of iterative enrichment and amplification (Ellington, 1994; Gold, 1995) (Figure 1). SELEX has been shown to be a general method for generating ligands to a wide variety of targets, including small molecules, peptides, and proteins. Blended SELEX is the process of incorporating an extraneous molecule into a nucleic acid library and then selecting the most active of these composite assemblies. These extraneous small molecules extend the chemical power of the nucleic acid library. Looked at another way, each nucleic acid sequence in the starting library is a variant of the small molecule moiety; blended SELEX allows up to 10^{15} variants of the small molecule to be screened for the most active variant.

The inhibitors recovered in the previous blended SELEX experiment showed good activity, with second-order rate constants for human NE inactivation of $\sim 3 \times 10^6$ M^{-1} min^{-1} and excellent specificity for NE as opposed to similar serine proteases, such as cathepsin G (Smith et al., 1995). The

* To whom correspondence should be addressed.

[⊗] Abstract published in *Advance ACS Abstracts,* February 15, 1997.

[1] Abbreviations: valP, diphenyl-(*R*)-1-amino-2-methylpropanephosphonate; NE, neutrophil elastase; hNE, human neutrophil elastase; α-1 PI, alpha-1 proteinase inhibitor; ARDS, acute respiratory distress syndrome; SELEX, Systematic Evolution of Ligands by Exponential enrichment; NHS, *N*-hydroxysuccinimide; SDS, sodium dodecyl sulfate; TEA, triethylamine; HBSS, Hank's balanced saline solution; hSA, human serum albumin; TBE, Tris/borate/EDTA; EDTA, ethylenediaminetetraacetate; PCR, polymerase chain reaction; AAPV, Ala-Ala-Pro-Val; pNA, *para*-nitroanilide; AMC, 7-aminomethylcoumarin; PAGE, polyacrylamide gel electrophoresis.

S0006-2960(96)02669-4 CCC: $14.00

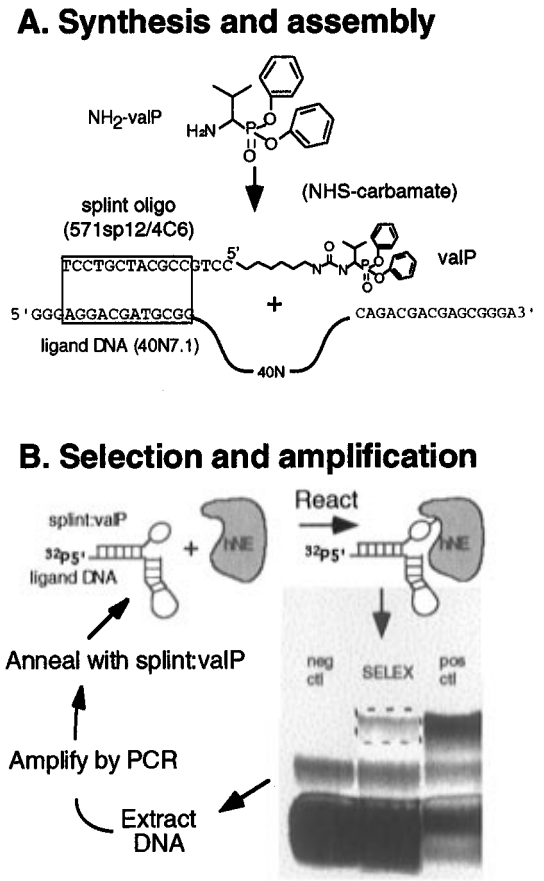

FIGURE 1: Chemistry and SELEX. (A) The core inhibitor, NH_2-valP is shown. This molecule was activated *via* an NHS-ester derivative and coupled to the amino linker of the splint oligo, as described in Methods. The splint oligo is complementary to 12 nt of the 5′ fixed region of the randomized DNA library. The complete inhibitor is assembled by annealing the splint oligo:valP conjugate to the DNA library. (B) Selection: the assembled inhibitors are incubated with a limiting amount of hNE, and the valP moiety reacts covalently with hNE. These covalently coupled complexes are resolved from unreacted inhibitor by SDS−PAGE. The shifted DNA is extracted and amplified by PCR for the next cycle of selection.

inactivation rates of the blended SELEX inhibitors are comparable to the best peptide inhibitors employing the phosphonate chemistry. We also showed these inhibitors to be effective in preventing lung damage in an *ex vivo* model of ARDS.

We have repeated the blended SELEX process with the goals of (a) recovering much more potent inhibitors, (b) recovering smaller and thus easier-to-synthesize ligands, and (c) selecting for *in vivo* potency by using activated neutrophils as the source of NE and thus mimicking the physiological milieu.

We describe in this paper the isolation and characterization of DNA-based inhibitors of NE that have inactivation rate constants of up to 3×10^8 M^{-1} min^{-1}, a rate significantly faster than that reported for any other irreversible inhibitor of NE. Two ligands cross-react quite well with rat NE (inactivation rate $\geq 10^8$ M^{-1} min^{-1}), which will facilitate testing in animal disease models. These ligands can be reduced in size from 71 nucleotides (nt) to 42−48 nt, while retaining inactivation rate constants greater than 3×10^7 M^{-1} min^{-1}. The inhibitors are shown to be 5−8 times more potent than the endogenous NE inhibitor, α-1 PI, at inhibiting elastin degradation by activated human neutrophils *in vitro*.

Scheme 1

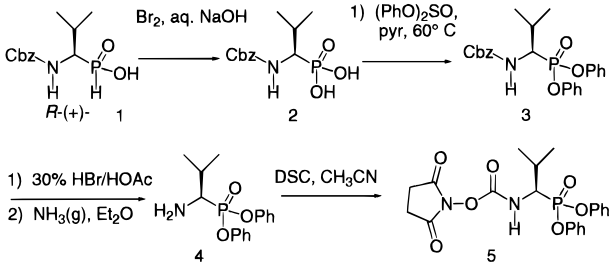

METHODS

Synthesis of Human Neutrophil Elastase Chiral Coligands for Splint SELEX

(*R*)-(−)-1-Benzyloxycarbonylamino-2-methylpropanephosphonic acid **2** was obtained by oxidation of the corresponding phosphonous acid **1** (Baylis et al., 1984) with bromine in aqueous base (Scheme 1). Conversion to the diphenyl ester **3** was accomplished in high yield utilizing diphenylsulfite in pyridine (Yamazaki et al., 1974). The crude diphenyl ester **3** was deprotected directly to the amine hydrobromide salt with 30% HBr/HOAc, which was purified by trituration with ether then converted to the amine **4** by treatment with ammonia gas (Oleksyszyn & Subotkowska, 1980). Subsequent transformation to the succinimidylcarbamate **5** was performed according to the method described previously (Smith et al., 1995).

Synthesis and Purification of Valine Phosphonate Enantiomers

valP conjugates were synthesized as follows: the triethylammonium salt of 571sp 12/4 C6 DNA (Figure 1) was dried under vacuum and resuspended in dry DMSO/10% TEA at a concentration of approximately 10 mg/mL. NHS-valP (**5**) (15 mg) was added (∼30-fold molar excess) and allowed to react at room temperature for 1 h, when the reaction was quenched by addition of 0.1 mL 1M Tris, pH 8.1. The modified DNA was purified by reverse-phase HPLC in a gradient of triethylammonium acetate/acetonitrile. The identity of the desired product was confirmed by electrospray ionization mass spectroscopy.

SELEX

SELEX procedures were performed largely as described (Smith et al., 1995), with the difference that DNA, rather than 2′NH_2-substituted RNA, libraries were used. Briefly, initial pools were composed of 100 pmol of chemically synthesized 40N7.1 DNA (Figure 2; high-salt SELEX) or DNA amplified from 25 pmol of synthetic DNA for 12 PCR cycles (neutrophil SELEX). DNA libraries were added to a 1.1-fold excess of DNA:valP splint in the reaction buffer at 0.1 μM (HBSS/0.01% hSA/25mM HEPES, pH 7.5, for neutrophil SELEX, the same buffer plus 100 mM NaCl for high-salt SELEX), and annealed by heating at 65 °C, followed by slow cooling to 37 °C. Neutrophils or purified hNE (Athens Research Technology, Athens, GA) and soluble elastin (Elastin Products Corp., Owensville, MO) were added and allowed to react. DNA was recovered from the neutrophil SELEX reactions by filtration through Spin-X 0.45 μm cellulose acetate filter cartridges (Costar, Cambridge, MA), followed by a wash with 0.05% SDS to remove any

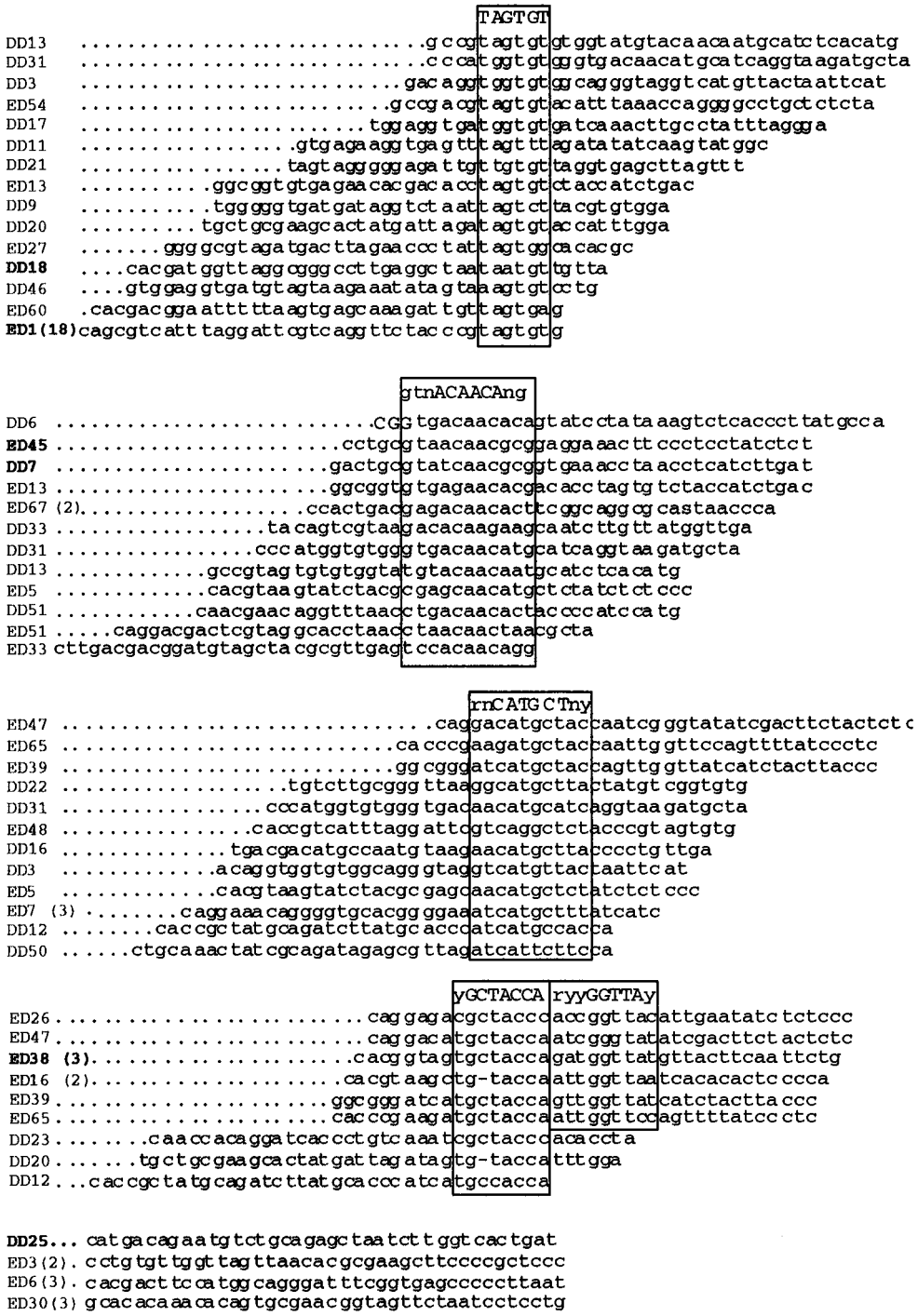

FIGURE 2: Local consensus in selected sequences. Sequences from the random region are aligned on local consensus sequences, shown in the boxes. r = purine, y = pyrimidine, n = any nucleotide. Sequences from the high-salt SELEX are denoted DD, sequences from the neutrophil SELEX are denoted ED. Sequences studied in more detail are in bold. Parentheses following the sequence names denote the number of clones isolated. The bottom group are sequences that did not fall into any of the groups, but were studied in more detail, or had multiple clones.

membrane-bound DNA. In the high-salt SELEX, the reactions were quenched by addition of SDS to 0.1%, and the reactions were concentrated and desalted by ultrafiltration through Centricon 30 kDa molecular weight cutoff cartridges (Amicon). Inhibitor:hNE conjugates were resolved from unreacted DNA by electrophoresis in a 6% polyacrylamide/0.05% SDS/1.5× TBE gel at 18 W constant (~300 V) for 2 h in a 4°C room. The amount of shifted DNA was quantified using a Fujix Phosphorimager, and then the DNA was cut out and eluted from the gel.

DNA for subsequent rounds was amplified by PCR using the 5′ fixed region primer 5N7.1C (5′-GGGAGGACGATGCGG) and the 3′ fixed region primer 3N7.1bio (5′-BBBTCCCGCTCGTCGTCTG, where "B" denotes biotin). The three biotins at the 5′ end of 3N7.1 cause the complement of the ligand strand to be retarded on a denaturing gel and so allow the ligand strand to be resolved and purified.

As the selections progressed, the stringency of the reaction conditions was increased in order to maintain selection pressure. For the high-salt SELEX, the initial conditions were 100 nM DNA, 10 nM hNE for 10 min. The final conditions were 10 nM DNA, 1.5 nM hNE, 400 μg/mL soluble elastin for 3 min. For the neutrophil SELEX the initial conditions were 90 pmol of DNA, 2.3 $\times$ 10^5

neutrophils in 75 μL for 5 min. The final conditions were 25 pmol of DNA, 3.8×10^4 neutrophils, 1000 μg/mL soluble elastin in 100 μL for 2 min. The amount of DNA shifted in each round was typically about 0.03, with a range 0.01−0.15. Soluble elastin was added as a competitor to increase the stringency of selection; pilot experiments showed that it inhibits hNE with a $K_{i\ app} \approx 70$ μg/mL (data not shown).

Round 15 DNA from the neutrophil SELEX and round 18 DNA from the high-salt SELEX were cloned by blunt-end ligation of PCR DNA into vector "PCR-script SK+" (Stratagene) and transformation into "Epicurian Competent SURE Cells" (Stratagene). DNA sequences were obtained by enzymatic sequencing.

Neutrophil Preparation. Blood drawn from human volunteers (20/mL) was layered on a discontinuous gradient of 12.5 mL each Histopaque 1077 and Histopaque 1119 (Sigma) in a 50 mL conical Falcon tube and centrifuged in a swinging bucket rotor at 400*g* for 30 min at room temperature. Neutrophils were drawn from the Histopaque 1077−1119 interface, and any contaminating red blood cells were hypotonically lysed by 30 s of vortexing in 3 mL of ice-cold water. Lysed cells and Histopaque were removed by washing cells three times in 20 mL HBSS containing no Ca^{2+} or Mg^{2+}. Neutrophils were resuspended in the same buffer, and their number and viability were determined by counting in 0.2% Trypan Blue.

Elastase activity of neutrophil preparations was determined using the AAPV−pNA microtiter plate assay (below). Typically, a series of dilutions of $(0.5-2) \times 10^5$ cells/well was activated by addition of 0.1 μg/mL phorbol myristyl acetate (Sigma) plus 0.5 μg/mL calcium ionophore A23187 (Sigma). Using purified hNE as a standard, elastase activity was typically about 2×10^{-17} mol/cell, with a range 2-fold higher or lower.

Enzymatic Assays

Small Molecule Assay. An elastase substrate *N*-methoxysuccinyl AAPV-pNA or *N*-methoxysuccinyl AAPV-AMC (Enzyme Systems Products, Dublin, CA) at 0.5 mM was mixed with inhibitor at the indicated concentration in 0.3 mL of HBSS/25 mM Tris, pH 7.5/0.01% hSA in a microtiter plate well at 37 °C. The reaction was initiated by adding hNE at 3 nM. AAPV-pNA reactions were monitored by absorbance at 405 nm in a BioTek EL312 microtiter plate reader. AAPV-AMC reactions were monitored by fluorescence ($\lambda_{ex} = 360$ nm, $\lambda_{em} = 460$ nm) in a Cytofluor II fluorescence microtiter plate reader (PerSeptive Biosystems, Framingham, MA). The data were fit (Kaleidagraph, Synergy Software) to eq 1:

$$A_{405} \text{ or FU} = v_0 \frac{(1 - e^{-k_{obs\ inact} t})}{k_{obs\ inact}} + A_t \qquad (1)$$

where FU is fluorescence units, v_0 is the initial rate of peptide hydrolysis, $k_{obs\ inact}$ is the observed rate of inactivation, and A_t is a displacement factor. This equation describes the behavior of an inhibitor which initially binds the enzyme rapidly and reversibly to attain a steady state, and subsequently reacts with first order kinetics to inactivate the enzyme. The rapid steady state assumption has been tested with first-generation SELEX elastase inhibitors.

The apparent second-order rate constant of inactivation, $(k_{inact}/K_I)_{app}$, was obtained by replotting $k_{obs\ inact}$ as a function of inhibitor concentration and determining the slope of the least-squares linear regression. To correct for competition between elastase substrate and inhibitor, the true second-order rate of inactivation was calculated using a model of full competitive inhibition:

$$\frac{k_{inact}}{K_I} = \frac{k_{inact}}{K_I}\text{app}\left(1 + \frac{[\text{AAPV-X}]}{K_{M\ AAPV-X}}\right)$$

The K_M values for both AAPV-pNA and AAPV-AMC were determined to be 100 μM both under standard assay conditions and in the absence of K^+; in the absence of M^{2+}, the AAPV-AMC K_M value rose to 160 μM (not shown).

Inhibition of rat neutrophil elastase was determined using a partially purified preparation from rat neutrophil granules (Athens Research), diluted to give activity equivalent to that used in the hNE assays. The K_M value of AAPV-AMC was determined to be 66 μM (not shown). Inhibition of human cathepsin G (Calbiochem) was determined using the substrate *N*-methoxysuccinyl AAPF-pNA (Calbiochem), with enzyme at 50 nM, and substrate at 0.5 mM. The K_M value for AAPF-pNA was determined to be >1 mM, and so no correction was made for competition between substrate and inhibitor.

Elastin Degradation Assay. The degradation of insoluble elastin by neutrophils was determined using elastin-fluorescein, particle size 37−75 μm (Elastin Products Company), as a substrate. Assays were performed in a 96-well format using Multiscreen-DP 0.65 μm PVDF filter plates (Millipore). Prewashed elastin-fluorescein at a final concentration of 1 mg/mL and inhibitor were mixed in the wells at 37 °C in HBSS/25 mM HEPES pH 7.5/0.01% hSA. Reactions were initiated by addition of neutrophils directly following activation with 0.1 μg/mL phorbol myristyl acetate plus 0.5 μg/mL calcium ionophore A23187. The number of neutrophils was calibrated by the AAPV-pNA assay to yield the equivalent of 50 nM purified hNE activity per well, typically $(1-2) \times 10^5$ neutrophils per well. The final volume of the reaction was 150 μL. Reactions were allowed to proceed for 1 h, then stopped by addition of 100 μL of 0.02% SDS. Solubilized elastin-fluorescein peptides were recovered by stacking the Multiscreen plate on a 96-well V-bottom plate and centrifuging at 1000*g* for 5 min at room temperature. The filtrate (150 μL) was transferred to a 96-well flat-bottom plate, and fluorescence was determined in each well. Pilot assays with purified hNE showed that the reaction was linear with respect to both time and hNE concentration in the range of experimental conditions used.

RESULTS

SELEX Strategy

In our previous report, we described a variation of the blended SELEX process which we called "splint SELEX" for the DNA-small molecule conjugate that is annealed to the nucleic acid library through complementary base-pairing, thereby forming a "splint" (Figure 1A). Once annealed to the randomized nucleic acid library, the library:splint assembly is iteratively selected for the sequences that are most active in forming conjugates with hNE (Figure 1B). While retaining this basic scheme, we made the following changes, which resulted in the selection of much more active inhibitors:

Use of a Chirally Resolved Phosphonate. Phosphonate protease inhibitors have always been synthesized as racemic mixtures at the aminoacyl α-carbon, forming what are the equivalent of L- and D-amino acids. It is expected that the NE active site is selective with respect to the chirality of the substrate, preferring the inhibitor which corresponds to the biological L-amino acid. We have subsequently confirmed this expectation: the L-amino-acid-equivalent inhibitor is four times more potent than the R (data not shown). The first-generation blended SELEX inhibitors were selected using a racemic mixture. We suspected that factors related to the use of mixed enantiomers might drive the selection dynamic to some extent. We desired instead that potentiation of inhibition be the only selection factor, and therefore resolved the more active enantiomer for use in the selection.

Selection for Shorter Ligands. Shorter ligand sequences are desirable in order to reduce the cost and difficulty of synthesis. We found with our first-generation ligands that any reduction of sequence size from the original 71-mer resulted in significant losses of activity (J.C. & D.S., unpublished results). Elastase has a high net positive charge, and nucleic acids are negatively charged, so it is expected that electrostatic contributions to binding will be significant. We found that inhibition by the first-generation ligands was extremely salt-sensitive, consistent with these expectations (J.C. & D.S., unpublished results). In an interaction dominated by electrostatics, a large nucleic acid might be at an advantage for maximizing the total number of charge−charge interactions and for reaching from the active site to sites of high net positive charge, such as the "arginine patch" on hNE. We reasoned that higher ionic strength during selection would weaken electrostatic binding interactions, and might thereby reduce the selective disadvantage of smaller binding motifs that depend primarily on hydrogen-bonding or hydrophobic interactions.

Selection Using Activated Neutrophils. Elastase activity is highly localized *in vivo* and exists in a microenvironment that might differ substantially from that of the purified enzyme in homogenous solution (Campbell & Campbell, 1988; Liou & Campbell, 1995; Weiss et al., 1986). There have also been reports that NE is expressed in a membrane-bound form that might be physiologically important (Allen & Tracy, 1995; Owen et al., 1995). For these reasons we decided to include a selection that used activated neutrophils as the source of NE.

In summary, two selections were performed, one against purified NE in high salt (high-salt SELEX), and the second selection was performed with elastase expressed from activated neutrophils in physiological salt concentration (neutrophil SELEX).

Selection of Elastase Inhibitors

Fifteen rounds of neutrophil SELEX and 18 rounds of high-salt SELEX were performed, using the parameters described in Methods. The stringency of the selections was increased in later rounds by reductions in ligand concentrations and reaction times, and by addition of soluble elastin as a competitor (see Methods). Roughly 12 rounds were required in the high-salt SELEX before significant increases in inhibitory activity of the pool occurred, while increased activity was apparent in the neutrophil SELEX after only a few rounds. Significant background levels of gel-shifted DNA were apparent in the later rounds of both SELEXes. These levels were reduced by counter-selection: DNA pools were run on gels in the absence of hNE, and the unshifted material was collected for amplification and further selection. The background can probably be attributed to DNA−DNA dimer formation, as the amount of background shift was dependent on the DNA concentration in the sample. The selections were terminated when no further increases in pool activity were observed over three rounds.

Sequence Analysis

A total of 49 isolates were sequenced from the high-salt SELEX; all of these are unique sequences. Sixty-two isolates were sequenced from the neutrophil SELEX pool; 34 of these are unique sequences. One sequence, ED1, is represented 18 times, accounting for 29% of all clones in the pool. All 18 clones are perfect copies, and there are no closely related sequences, suggesting that the activity of this clone is strongly dependent on its intact, exact sequence.

Inspection of the 5′ ends of the sequences reveals a structural feature of the clones, one that differs between the high-salt and neutrophil SELEXes. The splint oligo is designed to form a 12 bp duplex with the 5′ fixed region of the ligand DNAs, and leave a 4 nt "dangling end" that may or may not form a structure with the ligand DNA random region (Figure 1). As with the first-generation ligands, a large majority (39/62) of the neutrophil SELEX ligands extend the fixed-sequence double helix by 2 bp with the sequence 5′CA; three more use wobble pairing to extend the helix with the sequence 5′TA. In contrast, the 49 high-salt SELEX ligands prefer wobble pairing (5′TG = 17, 5′TA = 9) to Watson−Crick pairing (5′CA = 7) in forming the extension. The functional significance of this difference is not clear, as there is no systematic difference between the two sets of sequences in any of our assays (below). It is also unlikely that the difference originates in the stabilities of the splint−ligand assemblies under different salt conditions, as DNAs from both SELEXes were annealed under identical physiological salt concentrations. It is also notable that two highly similar sequences emerged from the two SELEXes. Ligands DD7 (high salt) and ED45 (neutrophil) are 70% identical (28/40 nt) overall, with a 16 nt region of perfect identity near the 5′ end. The number of differences between the sequences is too large to allow the similarity to be plausibly explained by cross-contamination between the two selections. Instead, the similarity argues that the SELEX process successfully sampled and selected the optimal sequences from large libraries.

We used a computer-assisted method of local sequence consensus alignment (B. Javornik, unpublished results) to organize the sequence data on the basis of small (6−7 nt) sequence motifs (Figure 2). Sequences (19/49) from the high salt SELEX, and 17/34 from the neutrophil SELEX fall into one of these groups. Several sequences belong to more than one group. The sequence motifs, with one exception, appear to be distributed randomly within the randomized region and between the high salt and neutrophil SELEXes. The exception is the sequence 5′GCTACCA, which is found in the 5′ half of the randomized region only in sequences from the neutrophil SELEX. In these ligands, the sequence

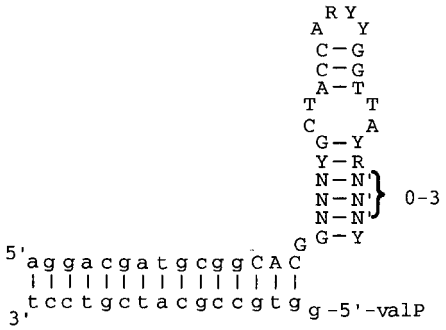

FIGURE 3: Neutrophil-specific structural motif. Fixed-region and splint oligo sequences are in lower case, random region sequence is in upper case. N−N′ denotes covarying base pairs.

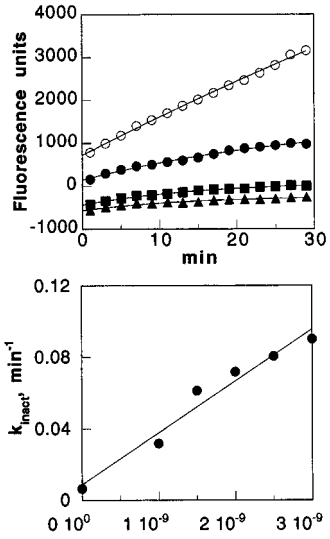

FIGURE 4: Fluorescence assay of hNE inactivation. (A) Progress curves of fluorescence intensity changes upon hydrolysis of the elastase substrate AAPV-AMC after subtraction from a no-enzyme control. ○, no inhibitor; ●, 1 nM ED1, ■; 1.5 nM ED1; ▲, 2 nM ED1. Only every other data point is shown for clarity. (B) Replot of inactivation rates from A. The value of $k_{inact\ obs}$ is calculated for each curve as described in Methods and replotted as a function of inhibitor concentration. Linear regression yields the apparent second-order rate of hNE inactivation, $k_{inact}/K_{I\ app}$. The true value for k_{inact}/K_I is obtained by correction for competition from hNE substrate, as described in Methods.

5′GGTTA is found 3′-ward. Computer-assisted folding analysis (Jaeger et al., 1989, 1990) shows that these two motifs may pair to form a hairpin with a 4 nt loop. The plausibility of this structure is supported by covariation analysis of the flanking sequences, which are able to extend this proposed hairpin by 3−6 bp (Figure 3). The restriction of this folding motif to the neutrophil SELEX suggests that it recognizes some neutrophil-specific epitope or isoform of hNE or is better adapted to function in the neutrophil microenvironment.

Inhibition of hNE

Fluorimetric Assay. Approximately 25 clones from each selection were prepared and assayed for hNE inhibition. These DNA:valine phosphonate complexes are irreversible inhibitors of elastase, and the rate at which they inactivate elastase is determined by the progress curve method (Figure 4). Because of the potency of the inhibitors, we used a fluorigenic substrate to maximize assay sensitivity, and allow low concentrations of enzyme and inhibitor to be used. To further slow the inactivation reaction to measurable rates, we used high concentrations of elastase substrate (0.5 mM, equal to 5 K_M), which competes with inhibitor for the enzyme active site and reduces the observed rate of inactivation.

Table 1: Inactivation Rate Constants

inhibitor	k_{inact}/K_I, M^{-1} min^{-1}
NH_2-valP	$3.8 \times 10^3 \pm 3.1 \times 10^2$
40N7.1	$1.8 \times 10^6 \pm 2.0 \times 10^5$
DD7	$2.2 \times 10^8 \pm 8.1 \times 10^7$
DD18	$1.1 \times 10^8 \pm 2.0 \times 10^7$
DD25	$9.2 \times 10^7 \pm 1.6 \times 10^7$
ED1	$1.5 \times 10^8 \pm 1.8 \times 10^7$
ED38	$9.9 \times 10^7 \pm 1.9 \times 10^7$
ED45	$1.0 \times 10^8 \pm 2.1 \times 10^7$

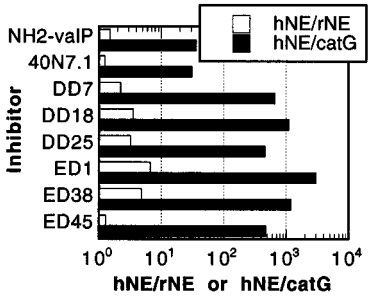

FIGURE 5: Inhibitor specificity. Values for k_{inact}/K_I were determined for rat NE and cathepsin G, as described in Methods, and plotted as the ratio of the values for human NE in Table 1. 40N7.1 is the starting DNA library.

The apparent second-order inactivation rates of the clones ranged from 10^7 to 2×10^8 M^{-1} min^{-1} (not shown). We chose three sequences from each selection for chemical oligonucleotide synthesis and more thorough characterization. These inhibitors have rates of $(1-3) \times 10^8$ M^{-1} min^{-1} (Table 1). These inactivation rates are approximately 100-fold faster than those of the starting pool. The rates also compare favorably with those of the best peptide phosphonate inhibitors ($\sim 2 \times 10^6$ M^{-1} min^{-1} (Oleksyszyn & Powers, 1991)) and the fastest irreversible inhibitors of any type previously reported (1×10^8 M^{-1} min^{-1} (Krantz et al., 1990)).

Specificity

Cross Reaction with Cathepsin G. Cathepsin G is a neutrophil serine protease that has similar substrate specificity to hNE, and like hNE, has a high net positive charge. We tested inactivation of cathepsin G as a measure of the discrimination of the inhibitors. The free valine phosphonate shows modest specificity, as does the random DNA:valP assembly; both inhibitors are 30- to 40-fold more active on hNE than on cathepsin G. In contrast, the selected inhibitors are 400- to 3000-fold more active against hNE than cathepsin G (Figure 5). ED1, the dominant sequence in the neutrophil SELEX pool, shows the greatest selectivity. The second-order rate constants of cathepsin G inactivation for the selected inhibitors are roughly the same as that of the unselected random pool, indicating that they were not selected on the basis of generally increased chemical reactivity.

Cross-Reaction with Rat NE. Several useful models of inflammatory disease have been developed in rat, so we screened our ligands for activity against rat neutrophil elastase, which has substrate specificity and structure similar to its human homologue (Virca et al., 1984). The free valine

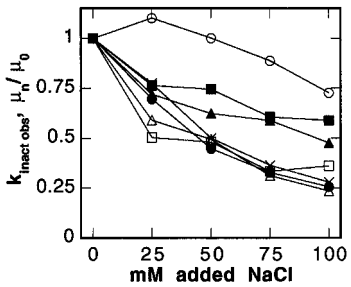

FIGURE 6: Salt sensitivity. $k_{inact\ obs}$ values for each inhibitor at the indicated salt concentration (μ_n) are normalized to its $k_{inact\ obs}$ value with no added salt (μ_0). The starting buffer, HBSS, is 142 mM in Na^+, and 6 mM in K^+. ×, 40N7.1 starting library; ●, DD7; ■, DD18; ▲, DD25; ○, ED1; □, ED38; △, ED45.

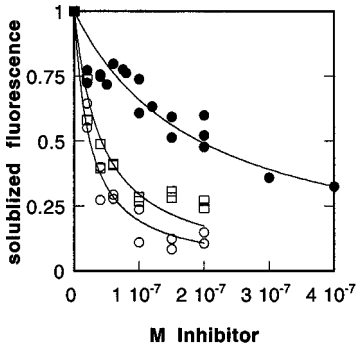

FIGURE 7: Inhibition of neutrophil-mediated elastin degradation. Activated neutrophils were incubated with fluoresceinated elastin, and degradation was quantified as the amount of solubilized fluorescence. Data were normalized to solubilized fluorescence with no inhibitor, minus solubilized fluorescence released in the absence of neutrophils. Data from two DNA-based inhibitors are shown, representing the lowest and highest IC_{50} values. ●, α-1PI; ○, DD7; □, DD25.

phosphonate and the random DNA:valP assembly have essentially the same reactivity against rat NE as against human NE (Figure 5). In contrast to cathepsin G, the selection process increased selectivity with respect to rat NE only slightly. As with cathepsin G, the most discriminating inhibitor is ED1, which is 6- to 7-fold more active against human NE than rat NE. Other ligands, notably DD7, and the closely related sequence ED45, are nearly as reactive against rat NE as against human NE, with inactivation rate constants approaching 10^8 M^{-1} min^{-1}.

Ionic Requirements

Salt Sensitivity. Our first-generation elastase inhibitors proved to be extremely sensitive to increases in ionic strength, as most of their inhibitory activity was lost upon addition of ≥50 mM NaCl to a physiological ionic strength buffer. As part of our strategy to recover smaller core sequences in inhibitors, we performed one selection at elevated ionic strength, adding 100 mM NaCl to a physiological buffer (HBSS). We tested the sensitivity of inhibitors from elevated- and physiological-ionic strength selections and found 3/6 have reduced sensitivity to increased ionic strength, while the others have similar sensitivity to that of randomized DNA (Figure 6). Two of these three are from the high-salt selection. Sequence ED1, from the neutrophil (*i.e.*, physiological ionic strength) selection, shows almost no sensitivity to increased ionic strength. The most sensitive inhibitor from the high-salt selection, DD7, is closely related to an inhibitor from the neutrophil selection, ED45.

K^+ Dependence. We further characterized the inhibitors with respect to K^+ dependence, which is diagnostic for the formation of G-quartet motifs in nucleic acid structures. Previously selected elastase-binding ligands were proposed to form G-quartets. The selection buffer contained ~6 mM K^+; this was replaced by Na^+ in the assays in order to maintain ionic strength. The inactivation rate constants of the free valyl phosphonate and of the randomized DNA:splint assembly show no significant change in the absence of K^+. Of the selected ligands, only DD18 and DD25 show significant (≥2 SEM) decreases in their inactivation rate constants in the absence of K^+. However, since the magnitude of the decrease is relatively small, 2- to 3-fold, this result suggests that the rate decrease is due to simple ionic selectivity, or that G-quartet structures are not critical to the inhibitors.

M^{2+} Dependence. Divalent cation binding sites are common in nucleic acid structures, commonly acting to stabilize tertiary interactions (Smith, 1995). Determination of inactivation rate constants shows that the closely related sequences DD7 and ED45 show modest (3- to 4-fold) reductions in activity in the absence of Ca^{2+} and Mg^{2+}.

Inhibition of PMN Degradation of Elastin. Determination of rate constants by use of small molecule substrate assays is useful in the kinetic characterization of inhibitors, but may be misleading with respect to evaluating their therapeutic potential (Padrines & Bieth, 1991). In contrast to the homogenous solution conditions of small molecule substrate assays, neutrophils in pathological conditions create a complex microscopic milieu of oxygen radicals and high enzyme concentration and adhere to an insoluble substrate. We developed an *in vitro* assay system which more closely resembles this milieu. Fresh, activated human neutrophils are incubated with fluoresceinated insoluble elastin, and elastinolysis is measured by the amount of soluble fluorescence produced. We measured the ability of our inhibitors to prevent elastinolysis over the course of an hour, in the presence of $(1-2) \times 10^5$ activated human neutrophils. Inhibition is quite efficient in this system for all the inhibitors, with IC_{50} values of 20−40 nM (Figure 7). It appears that all, or nearly all, of the neutrophil elastinolysis activity can be suppressed at higher (200 nM) concentrations of inhibitor. In contrast, the endogenous protease inhibitor α-1 PI is much less effective ($IC_{50} \approx 200$ nM), and it is not clear if α-1 PI can completely suppress elastinolysis.

Truncation Analysis

One of the goals of the second-generation SELEX was to obtain potent elastase inhibitors of shorter length to facilitate large-scale synthesis. We chose a set of inhibitors for truncation based on high activity, favorable location of local consensus sequence, and analysis of potential secondary structure. The three 5′-terminal nucleotides were removed from all truncates, leaving intact the full 12 bp splint-fixed region double helix. No more nucleotides were removed from the 5′ end, and progressively shorter inhibitors were synthesized by omission of 3′ terminal nucleotides. All sequences were initially synthesized with the 3′ fixed region removed, yielding inhibitors of length 51 or 52. The activity of all the inhibitors was reduced somewhat, with a range of 2- to 40-fold. Further truncation results in patterns of a sharp drop-off in activity, *e.g.*, DD7 and ED45, or a more gradual

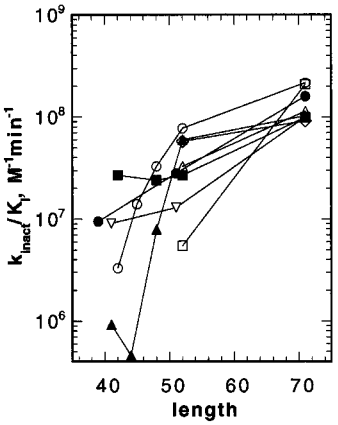

FIGURE 8: Truncation analysis. Second-order inactivation rates of inhibitors are replotted as a function of their length. All truncates have 3 nt removed from their 5′ end (see Figure 1), and all further truncation is by removal of nucleotides from the 3′ end. Parent sequences: ○, DD7; □, DD8; △, DD18; ▽, DD20; ◇, DD25; ●, ED16; ■, ED38; ▲, ED45.

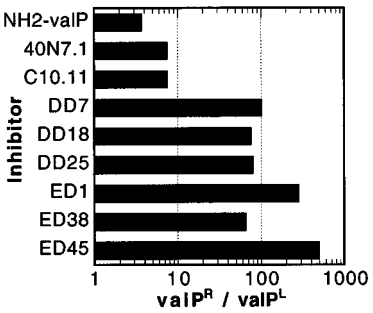

FIGURE 9: Chiral selectivity of inhibitors. Bars represent the ratio of inactivation rate constants for inhibitors as either the L- or D-amino acid form of the valine phosphonate moiety, denoted $valP^R$ and $valP^L$, respectively. NH_2-valP is the free valine phosphonate, and its ratio of ~4 represents the intrinsic selectivity of the valine phosphonate moiety. 40N7.1 is the randomized starting library. C10.11 is the best-characterized inhibitor from the first-generation SELEX, which was performed with an unresolved mixture of the L- and D- forms of the valine phosphonate.

loss in activity, *e.g.,* ED38 (Figure 8). The latter sequence has good activity at length 42 nt, with an inactivation rate constant of $\sim 3 \times 10^7$ M^{-1} min^{-1}, and is being used in further studies of elastase inhibition.

Enantiospecificity

One of the premises of our selection strategy was that our ligands would be sensitive to the chirality of the valine phosphonate moiety. We expected that use of a single enantiomer would result in the selection of ligands optimized to use that enantiomer. We tested this expectation by synthesizing and assaying a splint oligo which has the less-active enantiomer ($valP^L$, which corresponds to the D-amino acid) as the valine phosphonate moiety. Figure 9 shows that as free amine compounds, there is only a 4-fold difference between the enantiomers. Coupling to a splint oligo and annealing to randomized DNA (40N7.1) increases this distinction only slightly. The most-active ligand from the first-generation SELEX (C10.11), which was selected using the racemic mixture, shows no more enantiospecificity than the random DNA. In contrast, all of the second-generation ligands, which were selected using the pure $valP^R$ enantiomer (which corresponds to the L-amino acid), show a marked preference for this enantiomer, ranging in magnitude from 60- to 500-fold.

DISCUSSION

We previously reported the use of blended SELEX technology in the selection of elastase inhibitors. Blended SELEX incorporates a small molecule lead compound into a nucleic acid library and then applies the SELEX procedure to select the most active complex of small molecule and nucleic acid. The selections reported here were undertaken to further this work by producing highly potent elastase inhibitors that are especially adapted to the *in vivo* microenvironment of elastase activity and which could be reduced to a size more suitable for chemical synthesis. A combination of strategies were used in pursuit of these goals, as described in Results, and evaluated below.

Possibly the most important difference between the first- and second-generation blended SELEX elastase inhibitors is the use of a single-enantiomer small molecule inhibitor for incorporation into the SELEX library. Use of a racemic mixture in the first-generation SELEX might well have precluded the selection of sequences which interact strongly and specifically with the inhibitor moiety. Use of a single enantiomer in the second-generation SELEX resulted in the selection of inhibitors which are specific for the enantiomer used (Figure 9). It seems likely that as a consequence of this difference, the second-generation ligands are far more active as inhibitors, both in absolute terms (5×10^6 M^{-1} min^{-1} *vs* 3×10^8 M^{-1} min^{-1}) and in reference to increased activity over the starting pool (25- *vs* 130-fold). There are no apparent sequence similarities between the first- and second-generation ligands. Although this could be the result of the different selection conditions, it could also be the result of the different nucleic acid chemistries employed (pyrimidine 2′-NH_2 RNA *vs* DNA).

The effects of using high salt to de-emphasize electrostatic interactions and concomitantly to reduce the length of the ligand core sequence are unclear. Eight ligand sequences were studied in truncated forms. All ligands lost some degree of activity upon truncation and there appears to be no systematic difference between the high-salt and neutrophil (physiological salt) SELEXes. Furthermore, there is not even a clear distinction between the two selected pools with respect to salt sensitivity (Figure 6). Although 2 of the 3 high-salt SELEX ligands tested have reduced salt sensitivity, the least-sensitive ligand was produced by the neutrophil SELEX. It appears from this result that, despite the weakening of electrostatic interactions by addition of salt, these interactions were still powerful enough to contribute significantly to the DNA−elastase interaction and drive the selection.

Another approach to improving the properties of our elastase inhibitors was to select inhibitors for their activity against elastase expressed from activated human neutrophils. Because elastase activity is highly localized *in vivo*, we hoped to obtain ligands that are intrinsically more efficacious *in vivo* than inhibitors selected for their activity against purified enzyme in homogenous solution. Sequence and structural analysis (Figures 2 & 3) indicate that a neutrophil-specific class of ligands was selected by this approach. We tested ligands from both the neutrophil and high-salt SELEXes for their ability to inhibit elastin degradation by

activated neutrophils (Figure 7). All of the ligands were quite potent inhibitors of elastin degradation, with IC_{50} values in the range 20−40 nM. It appears that all, or nearly all, of the elastin degradation activity can be suppressed by our inhibitors, despite the participation of other proteases and oxygen radicals in elastin degradation (McGowan, 1990; Weiss et al., 1986). The endogenous inhibitor of elastase, α-1 PI, is much less effective in this assay, with an $IC_{50} \approx$ 200 nM. There is no significant difference between the IC_{50} values of ligands from the high-salt and neutrophil SELEXes in this assay. However, any differences might be masked by the relatively high amounts of elastase activity used in the assay. Neutrophils were added to give elastase activity equivalent to 50 nM NE in the small molecule assay; the IC_{50} values of ∼30 nM suggest that the system is near saturating concentrations for the elastase-inhibitor reactions.

Despite these ambiguities and the variable successes of our selection approaches, it is clear that we have produced extremely potent inhibitors of NE. The inactivation rate constants of the full-length ligands are $(1-2) \times 10^8$ M^{-1} min^{-1}. This rate is a few-fold less than the association constant for pseudoirreversible inhibition of hNE by α-1 PI, 5×10^8 M^{-1} min^{-1} (Ogushi et al., 1988), but compares favorably with other synthetic irreversible inhibitors: 7×10^7 M^{-1} min^{-1} for an isocoumarin (Kerrigan et al., 1995), 1×10^8 M^{-1} min^{-1} for a benzoxazin (Krantz et al., 1990), 5×10^7 M^{-1} min^{-1} for a benzoisothiazolone (Desai et al., 1995), 10^7 M^{-1} min^{-1} for a fluoroketone (Govardhan & Abeles, 1990). The power of the blended SELEX process to enhance the potency of small molecule is illustrated by comparison with peptidic valine phosphonate inhibitors: the best molecules of this class have inactivation rate constants of 2×10^6 M^{-1} min^{-1} (Oleksyszyn & Powers, 1989, 1991). Starting from the same valine phosphonate core, blended SELEX is able to produce far more potent inhibitors than have been produced by medicinal chemistry.

ACKNOWLEDGMENT

We thank David Tinnemeier (mass spec analysis), Tim Romig (HPLC), Ying Chang (sequencing), and Brenda Javornik (sequence analysis) for invaluable and expert assistance. We also thank Drs. Matthew Wecker, Torsten Wiegand, Larry Gold, and Bruce Eaton for critical reading of the manuscript.

REFERENCES

Allen, D. H., & Tracy, P. B. (1995) *J. Biol. Chem. 270*, 1408−15.
Baylis, E. K., Campbell, C. D., & Dingwall, J. G. (1984) *J. Chem. Soc., Perkin Trans. 1*, 2845−2853.
Birrer, P. (1993) *Agents Actions Suppl. 40*, 3−12.
Campbell, E. J., & Campbell, M. A. (1988) *J. Cell. Biol. 106*, 667−76.
Desai, R. C., Court, J. C., Ferguson, E., Gordon, R. J., Hlasta, D. J., Dunlap, R. P., & Franke, C. A. (1995) *J. Med. Chem. 38*, 1571−4.
Donnelly, S. C., MacGregor, I., Zamani, A., Gordon, M. W., Robertson, C. E., Steedman, D. J., Little, K., & Haslett, C. (1995) *Am. J. Respir. Crit. Care Med. 151*, 1428−33.
Doring, G. (1994) *Am. J. Respir. Crit. Care Med. 150*, S114−7.
Edwards, P., & Bernstein, P. (1994) *Med. Res. Rev. 14*, 127−94.
Ellington, A. D. (1994) *Curr. Biol. 4*, 427−9.
Gadek, J. (1992) *Am. J. Med. 92*, 27S-31S.
Gold, L. (1995) *J. Biol. Chem. 270*, 13581−13584.
Govardhan, C., & Abeles, R. (1990) *Arch. Biochem. Biophys. 280*, 137−46.
Hubbard, R. C., Fells, G., Gadek, J., Pacholok, S., Humes, J., & Crystal, R. G. (1991) *J. Clin. Invest. 88*, 891−7.
Jaeger, J., Turner, D., & Zuker, M. (1989) *Proc. Natl. Acad. Sci. U.S.A. 86*, 7706−7710.
Jaeger, J., Zuker, M., & Turner, D. (1990) *Biochemistry 29*, 10147−10158.
Jochum, M., Machleidt, W., & Fritz, H. (1993) *Agents Actions Suppl. 42*, 51−69.
Kerrigan, J. E., Oleksyszyn, J., Kam, C. M., Selzler, J., & Powers, J. C. (1995) *J. Med. Chem. 38*, 544−52.
Kramps, J. A., Rudolphus, A., Stolk, J., Willems, L. N., & Dijkman, J. H. (1991) *Ann. NY Acad. Sci. 624*, 97−108.
Krantz, A., Spencer, R., Tam, T., Liak, T., Copp, L., Thomas, E., & Rafferty, S. (1990) *J. Med. Chem. 33*, 464−79.
Liou, T., & Campbell, E. (1995) *Biochemistry 34*, 16171−16177.
McGowan, S. (1990) *Am. J. Respir. Cell. Mol. Biol. 2*, 271−9.
Ogushi, F., Hubbard, R. C., Fells, G. A., Casolaro, M. A., Curiel, D. T., Brantly, M. L., & Crystal, R. G. (1988) *Am. Rev. Respir. Dis. 137*, 364−70.
Oleksyszyn, J., & Subotkowska, L. (1980) *Synthesi*, 906.
Oleksyszyn, J., & Powers, J. (1989) *Biochem. Biophys. Res. Commun. 161*, 143−9.
Oleksyszyn, J., & Powers, J. (1991) *Biochemistry 30*, 485−93.
Ossanna, P. J., Test, S. T., Matheson, N. R., Regiani, S., & Weiss, S. J. (1986) *J. Clin. Invest. 77*, 1939−51.
Owen, C. A., Campbell, M. A., Sannes, P. L., Boukedes, S. S., & Campbell, E. J. (1995) *J. Cell. Biol. 131*, 775−89.
Padrines, M., & Bieth, J. G. (1991) *Am. J. Respir. Cell Mol. Biol. 4*, 187−93.
Powers, J., Odake, S., Oleksyszyn, J., Hori, H., Ueda, T., Boduszek, B., & Kam, C. (1993) *Agents Actions Suppl. 42*, 3−18.
Repine, J. (1992) *Lancet 339*, 466−9.
Smith, D. (1995) in *The Biological Chemistry of Magnesium* (Cowan, J., Ed.) pp 111−136, VCH Publishers, New York.
Smith, D., Kirschenheuter, G., Charlton, J., Guidot, D., & Repine, J. (1995) *Chem. Biol. 2*, 741−750.
Umeki, S., Niki, Y., & Soejima, R. (1988) *Am. J. Med. Sci. 296*, 103−6.
Virca, G., Metz, G., & Schnebli, H. (1984) *Eur. J. Biochem. 144*, 1−9.
Weiss, S. J., Curnutte, J. T., & Regiani, S. (1986) *J. Immunol. 136*, 636−41.
Yamazaki, N., Higashi, F., & Niwano, M. (1974) *Tetrahedron 30*, 1319−1321.

BI962669H